[PROC. OF JSCE No. 344/I-1 (Structural Eng./Earthquake Eng.) April 1984]

SPECTRAL CHARACTERISTICS OF BEDROCK MOTION IN THE TOKYO METROPOLITAN AREA

*By Shigeo KINOSHITA**

Based upon the direct measurement of bedrock motions, we proposed two models to predict the zero-damped velocity response spectra in the bedrock of the Tokyo metropolitan area for the period range from 0.1 to 10 s. These models were derived separately analyzing acceleration records of category A and category B earthquakes. Category B earthquakes distributed in and around the Philippine Sea plate. The response spectra predicted from the two models differ several times at the periods around 0.5 s for the same earthquake magnitude and hypocentral distance, while they come closer together at the periods longer than 1 s. Proper prediction of the bedrock motion is impossible for this area so far as a single model is used, where all earthquakes are mixed up.

1. INTRODUCTION

The surface ground motion due to an earthquake is estimated from the motion of the bedrock by convoluting the effects of the surface layer on the bedrock[1]. In Japan, the pre-Tertiary basement has been recognized as seismic bedrock. In the Tokyo metropolitan area, however, the pre-Tertiary basement, i.e., seismic bedrock, is covered with a thick sedimentary layer with a thickness of several kilometers[2].

Therefore, the deep down-hole observation of strong seismic motions is of particular importance in this area for prediction of the ground motion at the time of a large earthquake. The National Research Center for Disaster Prevention (NRCDP) constructed three seismographic observatories in and around Tokyo, and each site has a deep observation well[3]. The well bottom, where sensors including a three-component set of force balance accelerometer have been installed, is in the bedrock where the average velocity of normally propagating S wave has been directly measured as being about 2.5 km/s[4),5)].

Based upon the results of down-hole observation, we propose some models to predict zero-damped velocity response spectra, as an upper-bound estimate of Fourier amplitude spectra, of horizontal acceleration in the bedrock when earthquake magnitude and hypocentral distance are specified.

2. OBSERVATION METHOD AND DATA

Acceleration records analyzed in this study were obtained at the three observation sites which are shown in Fig. 1; IWT (Iwatsuki, Saitama Prefecture; 35°55′33″ N, 139°44′17″ E), SHM (Shimohsa, Chiba Prefecture; 35°47′36″ N, 140°01′36″ E), and FCH (Fuchu, Tokyo; 35°39′02″ N, 139°28′25″ E). Sensors were installed at the bottom of boreholes with depths of 3510 m at IWT, 2310 m at SHM, and 2750 m at FCH. Those depths are 600 m or

* Member of JSCE, M. Eng., Research Engineer, National Research Center for Disaster Prevention (Tennodai 3-1, Sakura-mura, Niihari-gun, Ibaraki-ken 305, Japan.)

more below the top of the pre-Tertiary basement. The cylindrical capsule installed at the bottom of boreholes contains the seismic and electronic equipment such as a three-component set of force balance accelerometer, amplifiers, an analog to digital converter, PCM transmitters, and a D. C. motor for controlling the balance of the seismometers. Such apparatuses are so designed to perfectly function under the severe circumstances of the well bottom, where temperature is 86°C and pressure is 350 atm in the case of IWT.

An electric signal from each accelerometer is fed to the amplifier having two output channels with different gains, and converted to the digital data (12 bit/sample) in the capsule. The digital data are transmitted by PCM method to the recording room on the ground surface. A wide dynamic range is covered by using the data from those two channels for each component. Maximum measurable accelerations are 16 and 327 gal for the high gain and the low gain channels, respectively. Over-all relative frequency characteristics are the same for the horizontal components. Fig. 2 shows the over-all frequency characteristics for the high gain channel. The frequency range of flat response in gain is from 0 to 10 Hz.

The data set used for this study consists of 60 horizontal component records of 24 earthquakes as shown in Fig. 1. Parameters of those earthquakes, which were determined by the Japan Meteorological Agency (JMA), are listed in Table 1 together with the

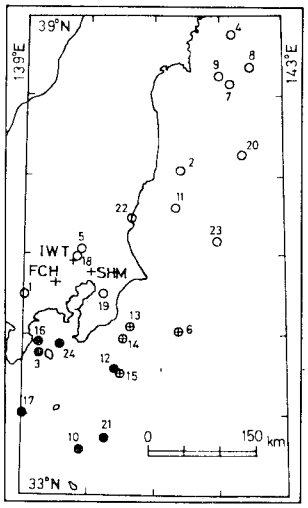

Fig. 1 Locations of observatories and epicenters. Observation sites are denoted by plus signs, epicenters of earthquakes in category A are denoted by open circles and those in category B by solid ones.

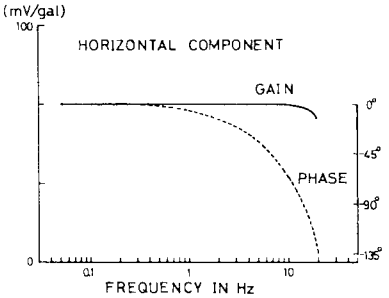

Fig. 2 Over-all frequency characteristics used for recording horizontal acceleration in the bedrock.

Table 1 Earthquake data used in the present study.

No.	Date	Latitude	Longitude	Depth (km)	Magnitude	Recording Site	Category
1	June 16, 1976	35° 30'	139° 00'	20	5.5	IWT	A
2	Oct. 6, 1976	37° 04'	141° 25'	70	5.9	IWT	A
3	Jan. 14, 1978	34° 46'	139° 15'	0	7.0	IWT	B
4	Feb. 20, 1978	38° 45'	142° 12'	50	6.7	IWT	A
5	Mar. 20, 1978	36° 05'	139° 53'	60	5.5	IWT	A
6	Apr. 7, 1978	35° 03'	141° 22'	30	6.1	SHM	
7	June 12, 1978	38° 09'	142° 10'	40	7.4	IWT, SHM	A
8	June 14, 1978	38° 21'	142° 29'	40	6.3	SHM	A
9	June 21, 1978	38° 15'	142° 00'	50	5.8	SHM	A
10	Oct. 11, 1978	33° 34'	140° 53'	50	5.7	SHM	B
11	July 11, 1979	36° 36'	141° 19'	40	5.9	IWT, SHM	A
12	Aug. 12, 1979	34° 35'	140° 23'	50	5.7	SHM	B
13	Oct. 28, 1979	35° 07'	140° 45'	90	5.5	SHM	
14	Mar. 12, 1980	34° 57'	140° 31'	80	5.6	IWT, SHM	
15	May 8, 1980	34° 31'	140° 27'	60	5.7	IWT, SHM	
16	June 29, 1980	34° 55'	139° 14'	10	6.7	IWT, SHM, FCH	B
17	Sep. 10, 1980	34° 01'	139° 00'	20	5.6	SHM	B
18	Sep. 24, 1980	35° 58'	139° 48'	80	5.4	IWT, FCH, SHM	A
19	Sep. 25, 1980	35° 31'	140° 13'	80	6.1	IWT, FCH	A
20	Apr. 13, 1981	37° 16'	142° 21'	30	5.7	FCH	A
21	Feb. 21, 1982	33° 43'	141° 14'	40	6.4	SHM, FCH	B
22	Mar. 7, 1982	36° 28'	140° 39'	60	5.5	SHM, FCH	A
23	July 23, 1982	36° 11'	141° 57'	30	7.0	SHM, FCH	A
24	Aug. 12, 1982	34° 53'	139° 34'	30	5.7	IWT	B

recording sites. Magnitude range is from 5.4 to 7.4, and hypocentral distance is from 65 to 385 km.

3. METHOD

We model the bedrock motion in the Tokyo metropolitan area by using the functional form :

$$SV(T)=10^{a(T)M-b(T)\log_{10}R+c(T)} \quad (1)$$

where $SV(T)$ is the zero-damped velocity response spectum (in cm/s) of the horizontal acceleration at the period T. M is magnitude, and R is hypocentral distance in km. The coefficients $a(T)$, $b(T)$, and $c(T)$ are given at each period T. The form of relation (1) has been used by many investigators to represent the spectral charactristics of bedrock motions[1)~8)]. A set of coefficients $a(T)$, $b(T)$, and $c(T)$ at each period of interest is calculated by applying the least squares method to the linear relation which is obtained by taking logarithms on both sides of the relation (1). The coefficients were computed for 41 points in the period range from 0.1 to 10 s.

4. ANALYSIS

As a result of regression analysis of the 60 records, the coefficients a, b, and c were obtained as shown by model I in Fig. 3. Making use of those coefficients and the relation (1), $SV(T)$ are estimated for each earthquake with the specified M and R. Figs. 4~11 compare thus the estimated $SV(T)$ and original $SV(T)$ for some of the earthquakes. These figures indicate that the $SV(T)$ predicted from model I are not satisfactory; the predicted $SV(T)$ are systematically lower than the original ones for the cases shown in Figs. 4~7, and systematically higher for the cases shown in Figs. 8~11. This systematic tendency is kept irrespective of the observational site for the same earthquake. This fact shows that it is not appropriate to lump together all the data for constructing a realistic prediction model.

Therefore, we classified the earthquakes for which model I resulted in the under-estimation of the original $SV(T)$ as category A and those which resulted in the over-estimation as category B. Thirteen earthquakes are classified into category A and seven earthquakes into category B, respectively. The number of records in category A is 32 and those in category B is 17. Only four earthquakes show fairly good concordance between the predicted and observed $SV(T)$ by model I (see Table 1). In Fig. 1, the epicenters of earthquakes in category B are shown by solid circles. It is interesting that those are earthquakes distributed in and around the Philippine Sea plate.

Coefficients a, b, and c were recomputed for the earthquakes of category A and category B, respectively. The results of the regression analysis are shown in Fig. 3 as models II and III, respectively. For the earthquakes

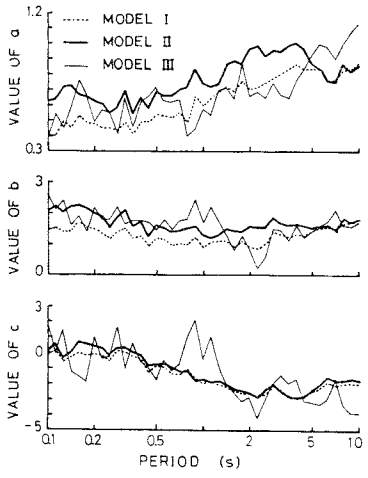

Fig. 3 Values of coefficients a, b, and c versus period, as calculated for the three models.

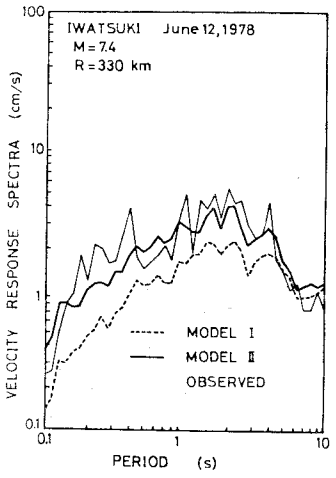

Fig. 4 Observed SV at IWT and SV estimated from models I and II.

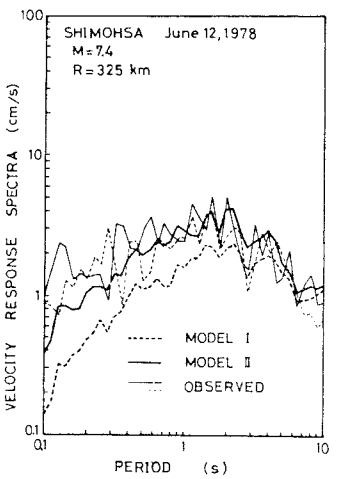

Fig. 5 Oversved SV for two horizontal components at SHM and SV estimated from models I and II.

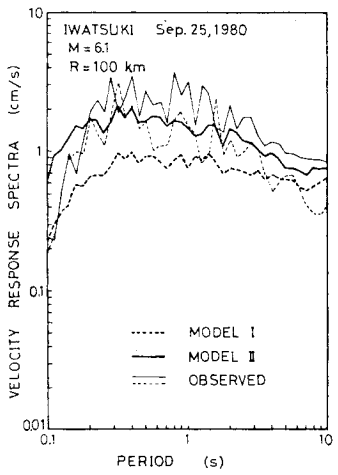

Fig. 6 Observed SV for two horizontal components at IWT and SV estimated from models I and II.

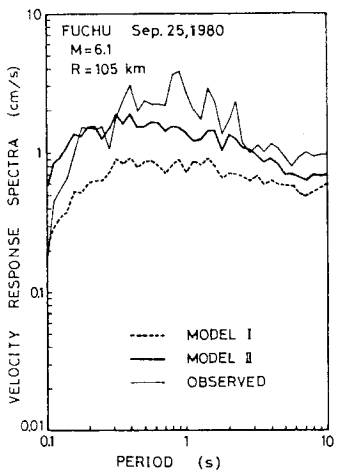

Fig. 7 Observed SV at FCH and SV estimated from models I and II.

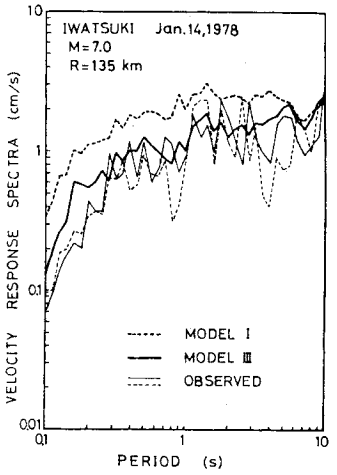

Fig. 8 Observed SV for two horizontal components at IWT and SV estimated from models I and III.

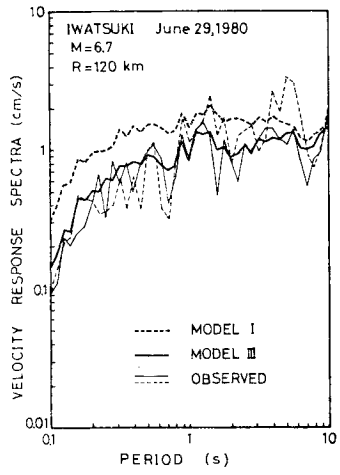

Fig. 9 Observed SV for two horizontal components at IWT and SV estimated from models I and III.

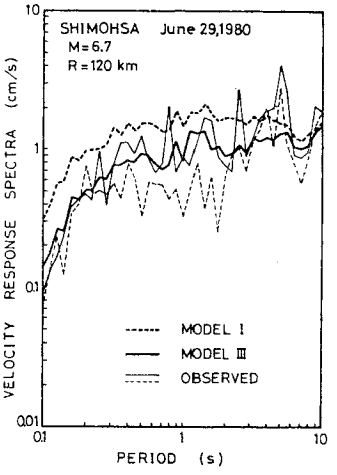

Fig. 10 Observed SV for two horizontal components at SHM and SV estimated from models I and III.

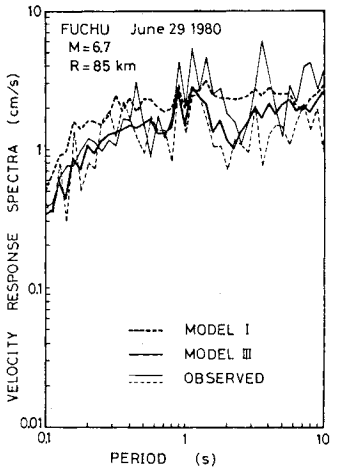

Fig. 11 Observed SV for two horizontal components at FCH and SV estimated from models I and III.

belonging to category A, the response spectra predicted from models I and II are compared with the obseved response spectra in Figs. 4 ~ 7. Similar comparisons between models I and III are shown in Figs. 8 ~ 11 for the earthquakes of category B. Those figures demonstrate that model II or model III is much better than model I in simulating the observed $SV(T)$. Fig. 12 shows the deviations of $|\log_{10}$ (observed $SV(T)$)-$\log_{10}$ (predicted $SV(T)$)$|$ for the three models. Comparing the deviations, it is understood that models II and III fit the observation much better than the preliminary single model, model I. Reasonably stable prediction of $SV(T)$ is expected from models II and III for a period longer than 0.2 s, and 1.0 s, respectively.

At two different observation sites of nearly the same hypocentral distance, the response spectra for the same earthquake show good concordance as can be seen comparing Figs. 4 and 5, Figs. 6 and 7, and Figs. 9 and 10. This fact may reflect that the three observatory's accelerometers are installed in common bedrock[3]. Fig. 13 shows the predicted $SV(T)$ for the magnitudes 5.4, 6.4, and 7.4 at the hypocentral distance of 80 km, for both models II and III. Figs. 14 and 15 are similar figures for the hypocentral distances of 160 and 320 km, respectively. These figures illustrate the change in the spectral shapes with respect to magnitude, hypocentral distance, and model. Two models

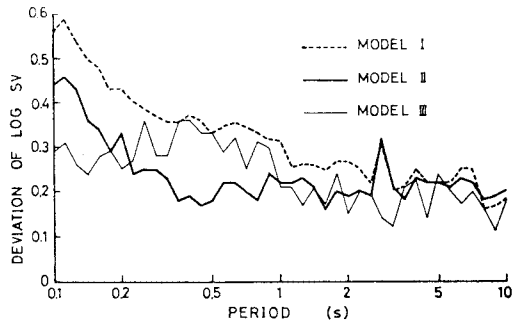

Fig. 12 Deviations of $\log_{10} SV$ versus period, as calculated for the three models.

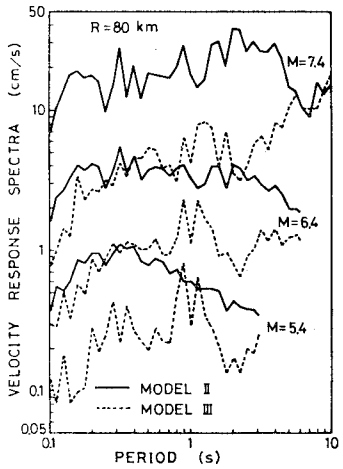

Fig. 13 SV of bedrock motion as a function of period predicted from models II and III for earthquakes of magnitude 5.4, 6.4, 7.4, and a hypocentral distance of 80 km.

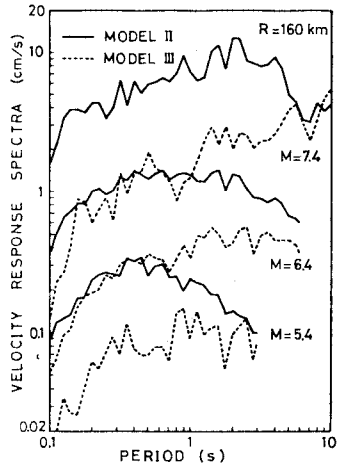

Fig. 14 SV of bedrock motion as a function of period predicted from models II and III for earthquakes of magnitude 5.4, 6.4, 7.4, and a hypocentral distance of 160 km.

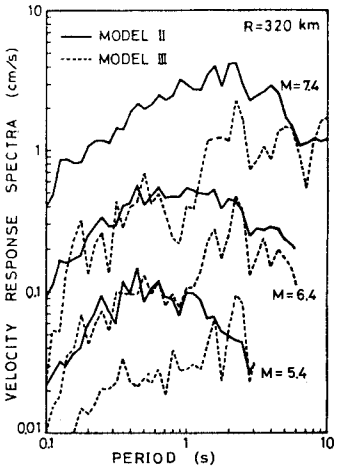

Fig. 15 SV of bedrock motion as a function of period predicted from models II and III for earthquakes of magnitude 5.4, 6.4, 7.4, and a hypocentral distance of 320 km.

have different spectral spapes. In case of model II, the spectral peak moves to a longer period with increase of magnitude. The $SV(T)$ predicted from model II are commonly larger than those of model III, the difference being several times at periods around 0.5 s. The difference between the two models, however, becomes small at periods longer than 1 s.

5. DISCUSSION

The JMA magnitude used in the present study was determined mainly by using displacement amplitudes which were recorded by the seismograph with the natural period of about 5 s. Fig. 16 shows frequency distribution of the period corresponding to the maximum displacement amplitude for the twenty four earthquakes studied. The data were obtained from the Seismological Bulletins of the JMA. It is seen from the figure that the JMA magnitude reflects the spectral density of seismic waves with periods of from 1 to 5 s for the magnitude range we investigated. This nature of the JMA magnitude explains the agreement of the $SV(T)$ predicted by models II and III at periods longer than 1 s, since spectral density at this period range should properly be reflected to the JMA magnitude.

For the shorter period, however, the $SV(T)$ predicted from model III (for category B earthquakes) are systematically small compared to those predicted from model II (for category A earthquakes), the difference being several times around 0.5 s. This contrast may be attributed to the path effect that the earthquakes of category B which are

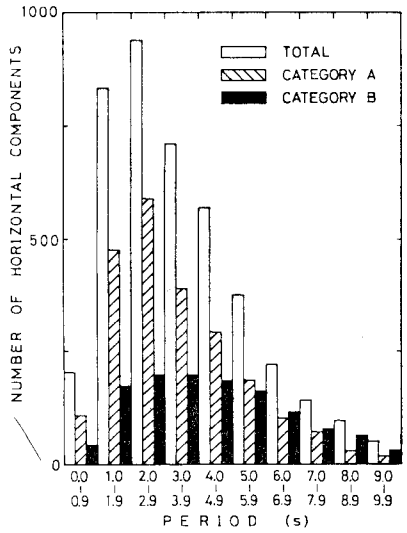

Fig. 16 Frequency distribution of the predominant period corresponding to the maximum displacement amplitude. Horizontal component records used were obtained by the seismographs installed in many observatories of the JMA for 24 earthquakes in Table 1.

distributed to the south of the observation sites (see Fig. 1) are affected by stronger attenuation during the propagation of seismic waves. Another possibility is difference in the source spectra between category A and category B earthquakes. Further studies from the viewpoint of seismology are needed to reveal which effect is dominant for the difference of the $SV(T)$.

6. CONCLUSION

Based upon the direct measurement of bedrock motions, we proposed two models to predict the zero-damped velocity response spectra in the bedrock of the Tokyo metropolitan area for the period range from 0.1 to 10 s. These models were derived separately analyzing acceleration records of category A and category B earthquakes in Fig. 1. The response spectra predicted from the two models differ several times at the periods around 0.5 s for the same earthquake magnitude and hypocentral distance, while they come closer together at periods longer than 1 s. Cause of the spectral difference for periods shorter than 1 s is open to future studies. We emphasize that proper prediction of the bedrock motion is impossible for the Tokyo metropolitan area so far as a single model is used, where category A and category B earthquakes are mixed up. The result obtained in the present report will be used as fundamental data for predicting the spectral characteristics of strong motions in the Tokyo metropolitan area, in connection with the effects of the thick sedimentary layer on the bedrock.

7. ACKNOWLEDGMENT

The author thanks Dr. M. Ohtake for advice and careful reading of the manuscript.

REFERENCES

1) Kanai, K. : Semi-empirical formula for the seismic characteristics of the ground, Bull. Earthq. Res. Inst., Tokyo Univ., Vol. 35, pp. 309~325, 1965.
2) Shima, E. : On the deep underground structure of Tokyo metropolitan area, Proc. 7 th Wld. Conf. Earthq. Engng. Istanbul, Turkey, 1980.
3) Takahashi, H. and Hamada, K. : Deep borehole observation of earth's crust activities around Tokyo-introduction of the Iwatsuki observatory, Pure and Appl. Geophys., Vol. 113, pp. 311~320. 1975.
4) Ohta, Y., N. Goto, Yamamizu, F. and Takahashi, H. : S-wave velocity measurements in deep soil deposit and bedrock by means of an elaborated down-hole method, Bull. Seism. Soc. Am., Vol. 70, pp. 363~377, 1980.
5) Yamamizu, F., Takahashi, H., Goto, N. and Y. Ohta : Shear wave velocities in deep soil deposits, Zisin, Vol. 34, pp. 465~479. 1981 (in Japanese).
6) McGuire, R. K. : A simple model for estimating Fourier amplitude spectra of horizontal ground acceleration, Bull. Seism. Soc. Am., Vol. 68, pp. 803~822, 1978.
7) Midorikawa, S. and Kobayashi, H. : Spectral characteristics of incident wave from seismic bedrock due to earthquake, Trans. Architect. Inst. Jpn., Vol. 273, pp. 43~54, 1978 (in Japanese).
8) Ohsaki, Y., Sawada, Y., Hayashi, K., Ohmura B. and Kumagai C. : Spectral characteristics of hard rock motions, Proc. 7 th Wld. Conf. Easthq. Engng, Istanbul, Turkey, 1980.

(Recieved August 26, 1983)